Three-dimensional CFD modeling of thermal behavior of a disc brake and pad for an automobile

Haydar Kepekci*, Ergin Kosa, Cüneyt Ezgi and Ahmet Cihan
Mechanical Engineering Department, Faculty of Engineering and Architecture, Beykent University, Ayazağa, Hadım Koruyolu Cd. No:19, 34398, Istanbul, Turkey

Abstract

The brake system of an automobile is composed of disc brake and pad which are co-working components in braking and accelerating. In the braking period, due to friction between the surface of the disc and pad, the thermal heat is generated. It should be avoided to reach elevated temperatures in disc and pad. It is focused on different disc materials that are gray cast iron and carbon ceramics, whereas pad is made up of a composite material. In this study, the CFD model of the brake system is analyzed to get a realistic approach in the amount of transferred heat. The amount of produced heat can be affected by some parameters such as velocity and friction coefficient. The results show that surface temperature for carbon-ceramic disc material can change between 290 and 650 K according to the friction coefficient and velocity in transient mode. Also, if the disc material gray cast iron is selected, it can change between 295 and 500 K. It is claimed that the amount of dissipated heat depends on the different heat transfer coefficient of gray cast iron and carbon ceramics.

Keywords: disc brake; CFD; modeling; transient; heat transfer

*Corresponding author: haydark-epekci@beykent.edu.tr

Received 15 January 2020; revised 12 March 2020; editorial decision 6 April 2020; accepted 6 April 2020

1 INTRODUCTION

The automobile disc brake is one of the essential safety components. It is subjected to many mechanical and thermal stresses during operation. According to the data obtained from the literature; shows that there is a high-temperature gradient ranging from 0 to 800°C due to friction between the buffer and the disc [1]. Disc brakes are mainly used to decelerate vehicles from the actual speed to the desired speed. During braking, mechanical energy is converted to heat due to friction [2].

After prolonged constant breaking, it can adversely affect the performance of the disc brake due to temperature rise and the change in friction properties due to overheating of the brake components. Also, other wheel suspension parts, such as the rim and tire, may be affected by high temperatures [3]. High temperatures during braking can cause premature wear, brake fluid evaporation, thermal cracking and vibration [4]. Therefore, it is crucial to estimate the temperature rise of the brake system and to evaluate the thermal performance of the brake system in the early design stage [5]. For a diesel engine automobile of 1400 cc, the front and rear of the disc brake and pad are illustrated in Figure 1.

There are many essential studies in the literature. Aderghal *et al.* [6] studied transient heat transfer in sliding connection experimentally and numerically. Kounas *et al.* [7] developed an analytical model for computing the coefficient of friction heat distribution among a rotating cylinder and a fixed pin. Laraqi *et al.* [8] suggested specific analytic resolutions to calculate the three-dimensional temperature distribution and the thermal contraction resistance caused by moving heat sources in semi-infinite bodies. Laraqi [9] used a feasible distribution of heat flux formation to calculate the coefficient of heat and flux separation produced by friction between the two layers. Moussa *et al.* [10] conducted experimental studies to determine the heat flow produced by the friction between the two floating bodies in perfect contact. Belhocine *et al.* [11] presented three-dimensional mathematical modeling to investigate the thermal performance of a

International Journal of Low-Carbon Technologies 2020, 15, 543–549

doi:10.1093/ijlct/ctaa022 Advance Access publication 28 May 2020

Figure 1. *The front and rear of the disc brake and pad.*

loaded and ventilated disc brake. Ghadimi *et al.* [12] studied the thermal analysis of a wheel-mounted disc brake. The disc brake and fluid zone were simulated as a 3D model with a thermal bonding boundary condition.

In the literature, computational fluid dynamics has been used in many studies on modeling. Some studies using CFD are as follows. Atmaca *et al.* studied a diesel evaporator that is a helical tube heat exchanger via roundabout heat provided by hot nitrogen gas which is modeled; the fractional distillation curve results of diesel fuel are compared with the experimental data reported in the literature. In their studies, they used ANSYS Fluent software, a commercial computational fluid dynamics program [13]. Atmaca *et al.* designed unmanned air vehicles and propellers of a UAV using computational fluid dynamics software. Its main objectives were turbulence, pressure and velocity changes which have been investigated. In their study, they used the ANSYS Fluent software in numerical analysis [14]. Atmaca studied wind tunnel experiments in buildings with different roof slopes. He did both numerical analysis and experimental work using the CFD program. He compared the data he obtained with each other. Numerical analysis data has shown that it is compatible with experimental results. As a result, he demonstrated the effect of the roof slope on the wind tunnel [15]. Atmaca and Ezgi modeled the steam ejector design and made numerical calculations using ANSYS Fluent software. They compared the results obtained from their calculations using energy equations for turbulent flow with the data in the literature [16].

In this study, an automobile that has a mass of 1800 kg is decelerated with an acceleration of 7 m/s^2 in 2 s. It has used three different speed limits determined for cars in traffic. The speeds are selected to be 50 km/h in built-up areas, 80 km/h on two lane roads (outside of built-up areas) and 120 km/h on highways/motorways. In this paper, calculations have been made by using two different disc materials. For each speed and each disc material separately, heat exchange graphs and temperature distribution on the surface disc brake system have been obtained. Thermal calculations based on the finite element method have been performed in transient mode by using computational fluid dynamics software. Experimental brake component tests, which were performed in ancient times, have now been replaced by simulation methods. These methods, based on thermal analyses using computational fluid dynamic (CFD) programs, have become popular in recent years. CFD programs are both economical and fast. They provide to inform about heat dissipation and heat dissipation rates of parts in detail. CFD analysis can be used at any stage of the process without the need for physical prototypes.

In this study, a disc brake and pad have been modeled and analyzed as 3D by a multi-physics software. The surface temperatures of the disc brake and the pad have been investigated to examine the maximum reached temperatures affecting the stability of pad and brake disc material at elevated values.

2 NUMERICAL METHOD

2.1 Governing equations

a. Power and pressure

The retardation power is

$$\dot{W} = -\frac{d}{dt}E_c = -\frac{d}{dt}\left(\frac{mV^2}{2}\right) = -mV\frac{dV}{dt} \tag{1}$$

For n brake:

$$\dot{W}_b = \frac{\dot{W}}{n} = -\frac{1}{n}mV\frac{dV}{dt} \tag{2}$$

The contact pressure between the disc and the pad is

$$P = \frac{Q_b}{\mu V} \tag{3}$$

where μ is the friction coefficient and Q_b is the heat rate.

$$Q_b = \frac{\dot{W}_b}{A} \tag{4}$$

b. Heat equation

$$\frac{1}{r}\frac{\partial}{\partial r}\left(kr\frac{\partial T}{\partial r}\right) + \frac{1}{r^2}\frac{\partial}{\partial \theta}\left(k\frac{\partial T}{\partial \theta}\right) + \frac{\partial}{\partial z}\left(k\frac{\partial T}{\partial z}\right) + \dot{q} = \rho c_p\frac{\partial T}{\partial t} \tag{5}$$

Since the disc is turning, the temperature gradient in the θ direction is negligible. If thermophysical properties are constant,

$$\frac{1}{r}\frac{\partial}{\partial r}\left(r\frac{\partial T}{\partial r}\right)+\frac{\partial^2 T}{\partial z^2}+\frac{\dot{q}}{k}=\frac{1}{\alpha}\frac{\partial T}{\partial t} \tag{6}$$

Produced and dissipated heat are expressed as

$$W_{\text{prod}}=\int_0^{t_0}\dot{q}_{\text{prod}}dt \tag{7}$$

$$W_{\text{diss}}=\int_0^{t_0}\dot{q}_{\text{diss}}dt \tag{8}$$

c. Thermal contact

The joint conductance is expressed as

$$h=h_{\text{c}}+h_{\text{g}}+h_{\text{r}} \tag{9}$$

where h_{c} is the constriction conductance, h_{g} is the gap conductance and h_{r} is the radiative conductance.

The constriction conductance is given by Cooper–Mikic–Yovanovich correlation,

$$h_{\text{c}}=1.25\,k_{\text{contact}}+\frac{m_{\text{asp}}}{\sigma_{\text{asp}}}\left(\frac{P}{H_{\text{c}}}\right)^{0.95} \tag{10}$$

where m_{asp} and σ_{asp} are the microscopic asperties. m_{asp} is the average slope, and σ_{asp} is the average height. P is the contact pressure, and H_{c} is the microhardness of the softer material. k_{contact} is the harmonic mean of the contacting surface conductivities.

The friction heat, Q_{fric}, is partitioned into 'rQ'_{fric} and $(1-r)Q_{\text{fric}}$ at the contact interface. If the two bodies are identical, r and $(1-r)$ would be 0.5, so that half of the friction heat goes to each surface. However, in the general case where the bodies are made of different materials, r is expressed by Charron's relation,

$$r=\frac{1}{1+\xi_{\text{d}}},\ \xi_{\text{d}}=\sqrt{\frac{\rho_{\text{u}}c_{p_{\text{u}}}k_{\text{u}}}{\rho_{\text{d}}c_{p_{\text{d}}}k_{\text{d}}}} \tag{11}$$

and symmetrically,

$$(1-r)=\frac{1}{1+\xi_{\text{u}}},\xi_{\text{u}}=\sqrt{\frac{\rho_{\text{d}}c_{p_{\text{d}}}k_{\text{d}}}{\rho_{\text{u}}c_{p_{\text{u}}}k_{\text{u}}}} \tag{12}$$

where u is the upside and d is the downside.

The heat fluxes at the upside (u) and downside (d) boundaries are

$$-n_{\text{d}}\,(-k_{\text{d}}.\nabla T_{\text{d}})=-h\,(T_{\text{u}}-T_{\text{d}})+r.Q_{\text{fric}} \tag{13}$$

$$-n_{\text{u}}.\,(-k_{\text{u}}.\nabla T_{u})=-h\,(T_{\text{d}}-T_{\text{u}})+(1-r)\,.Q_{\text{fric}} \tag{14}$$

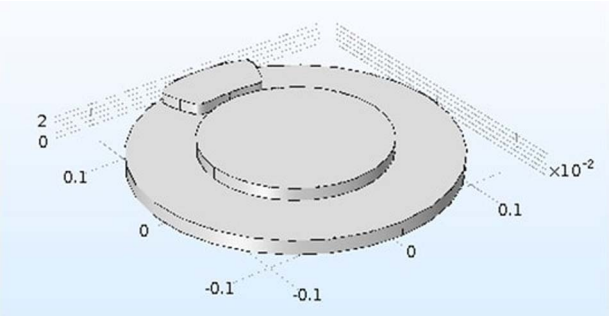

Figure 2. *General view of disc brake and pad.*

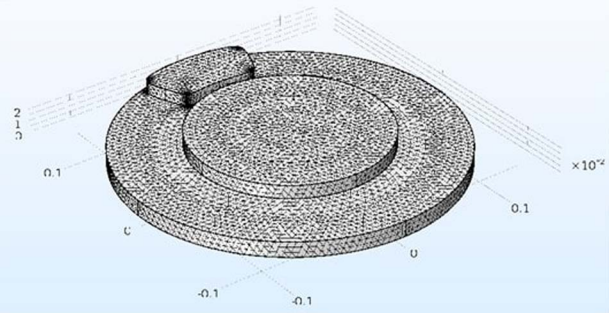

Figure 3. *General view of mesh prepared.*

2.2 CFD modeling of disc brake and pad

The 3D model of the disc brake system designed by taking convenient dimension values as in the previous studies of literature is given in Figure 2. The brake system is composed of the disc brake and pad components.

A simulation methodology has been examined on transient analysis of the temperature field in an automotive disc brake during and after a bustle brake movement that has the parameters used in the experimental study. It has been calculated at three different speeds, such as 50 km/h, 80 km/h and 120 km/h, and different frictional forces, such as 0.3, 0.5 and 0.7. After the computations are completed, the results are compared with each other.

The 3D mesh domain image of the disc brake analyzed is as shown in Figure 3. In CFD analysis, one of the criteria to be considered in order to reach the correct result is the number of mesh. When determining the number of mesh, $y+$ value is kept less than 1 to increase the accuracy. The number of cells contained in the mesh file created under these conditions was about 120,000.

The 3D model of the disc brake and pad geometry and their mesh have been modeled using CFD software. In the analysis, a PC with 'Intel (R) Core (TM) i7-4710HQ CPU @ 2.50GHz, four cores' has been used. The computational time took about 30 min. In the mesh file, the maximum element size was 0.0219, the minimum element size was 0.00027, the maximum element growth rate was 1.2, the curvature factor was 0.3 and the resolution of narrow regions was 0.5.

Table 1. *Parameters of the model.*

Inner disc diameter	137 [mm]
Outer disc diameter	80 [mm]
Disc thickness	11 [mm]
Pad thickness	10 [mm]
Initial vehicle speed	50–80–120 [km/h]
Deceleration	7 [m/s^2]
Wheel radius	0.25 [m]
Vehicle mass	1800 [kg]
Friction coefficient	0.3–0.5–0.7
Braking time (start)	0.5 [s]
Braking time (end)	2.5 [s]
Temperature, air	300 [K]

Table 2. *Properties of discs and pad.*

Thermo-physical properties	Disc 1	Disc 2	Pad
Material	Carbon ceramic	Gray cast iron	Composite material
Conductivity (W m $^{-1}$ K^{-1})	40	50	12
Density (kg m $^{-3}$)	1800	7200	2500
Heat capacity (J kg $^{-1}$ K^{-1})	800	447	900

The dimensions and operating conditions of the disc brake system taken from the literature are given in Table 1.

One of the disc materials is carbon ceramic; the other is gray cast iron. Also, the pad is made up of a composite material. The physical properties of the disc brake and pad material are given in Table 2.

The values used in the model are given to be σ_{asp} = 1 μm, m_{asp} = 0.4, H_c = 800Mpa, h_g = 0, h_r = 0.

The meshes are structured inside of the geometry. The purpose of the analysis is to calculate the surface temperature and dissipate and produce heat values at different velocities and different friction forces. As velocity values, 50, 80 km/h and 120 km/h have been selected. Also, friction coefficients have been selected to be 0.3, 0.5 and 0.7.

3 RESULTS

As can be seen in Figure 4, when the vehicle was moving at 50 km/h, after 2 s of braking, it has been observed that when the disc material carbon-ceramic has been selected, the disc brake and lining temperature increased to 370 K. If the disc material gray cast iron has been selected, this temperature has been observed to rise to 345 K. In the calculations, 0.3 has been chosen as a friction force.

As can be seen in Figure 5, when the vehicle was moving at 80 km/h, after 2 s of braking, it has been observed that when the disc material carbon-ceramic has been selected, the disc brake and lining temperature increased to 500 K. If the disc material gray cast iron has been selected, this temperature has been observed to rise to 420 K. In the calculations, 0.3 has been chosen as a friction force.

As can be seen in Figure 6, when the vehicle was moving at 120 km/h, after 2 s of braking, it has been observed that when the disc material carbon-ceramic has been selected, the disc brake and lining temperature increased to 650 K. If the disc material gray cast iron has been selected, this temperature has been observed to rise to 500 K. In the calculations, 0.3 has been chosen as a friction force.

As can be seen in Figure 7, when the vehicle was moving at 50 km/h, after 2 s of braking, it has been observed that when the disc material carbon-ceramic has been selected, the produced heat was 31621 J and dissipated heat was 78 J calculated. If the disc material gray cast iron has been selected, the produced heat was 31621 J and dissipated heat was 43 J.

As can be seen in Figure 8, when the vehicle was moving at 80 km/h, after 2 s of braking, it has been observed that when the disc material carbon-ceramic has been selected, the produced heat was 50117 J and dissipated heat has been calculated to be 250 J. If the disc material gray cast iron has been selected, the produced heat was 50117 J and dissipated heat was 158 J.

As can be seen in Figure 9, when the vehicle was moving at 120 km/h, after 2 s of braking, it has been observed that when the disc material carbon-ceramic has been selected, the produced

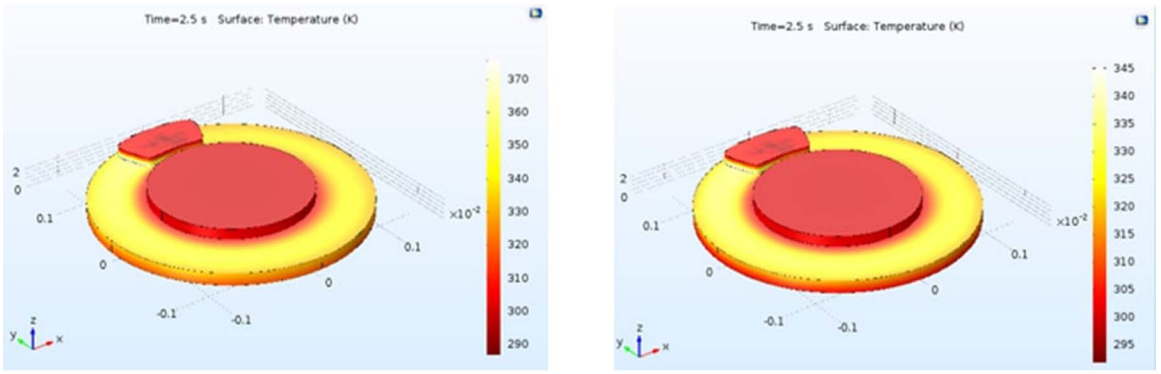

Figure 4. *The surface temperature of disc brake and pad for 50 km/h. (**a**) Carbon-ceramic, (**b**) gray cast iron.*

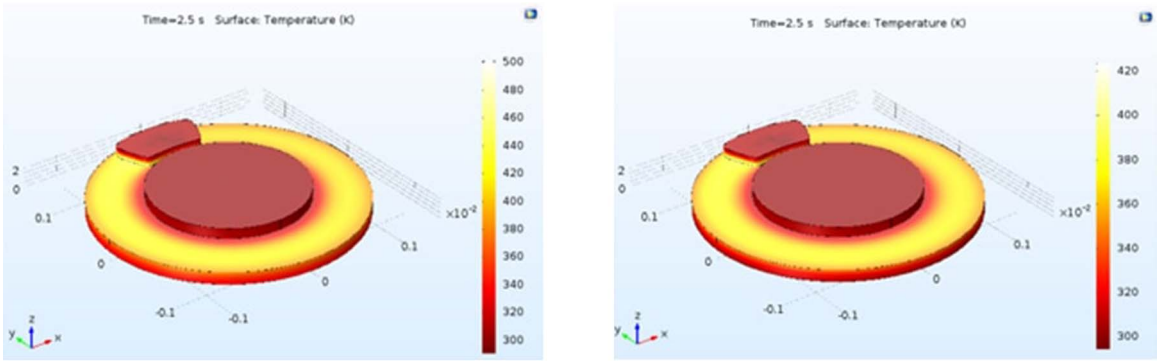

Figure 5. *The surface temperature of disc brake and pad for 80 km/h. (a) Carbon-ceramic, (b) gray cast iron.*

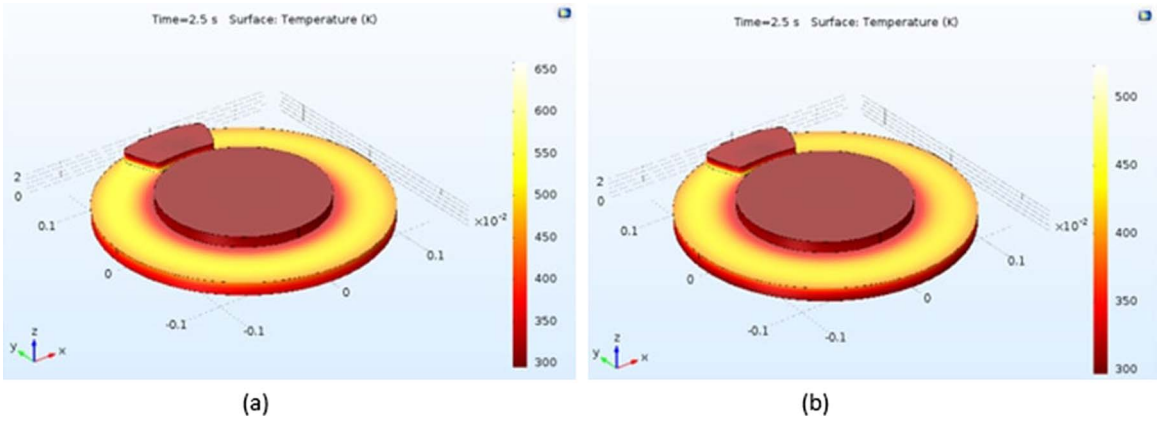

Figure 6. *The surface temperature of disc brake and pad for 120 km/h. (**a**) Carbon-ceramic, (**b**) gray cast iron.*

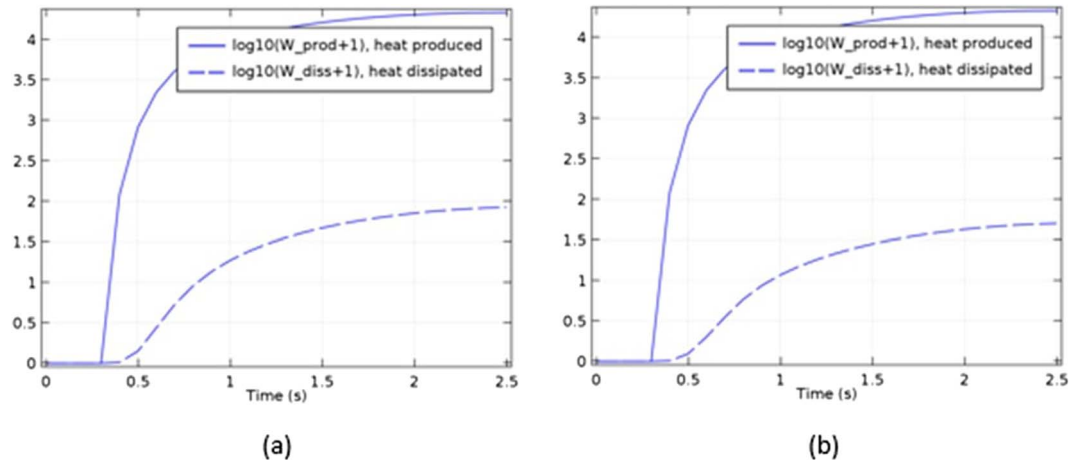

Figure 7. *Dissipated and produced heat (J) for 50 km/h. (**a**) Carbon-ceramic, (**b**) gray cast iron.*

heat was 79431 J and dissipated heat was 561 J calculated. If the disc material gray cast iron has been selected, the produced heat was 79431 J, and dissipated heat was 315 J.

As can be seen in Figure 10, the acceleration of a vehicle moving at constant speed decreases to -7 m/s^2 with 2 s of braking. It has been observed that the acceleration-time graph obtained from all analyses was the same.

The results have shown that the surface temperatures have been ranked for carbon-ceramic between 290–370, 300–500 and 300–650 K for the velocities of 50, 80 and 120 km/h, respectively. If

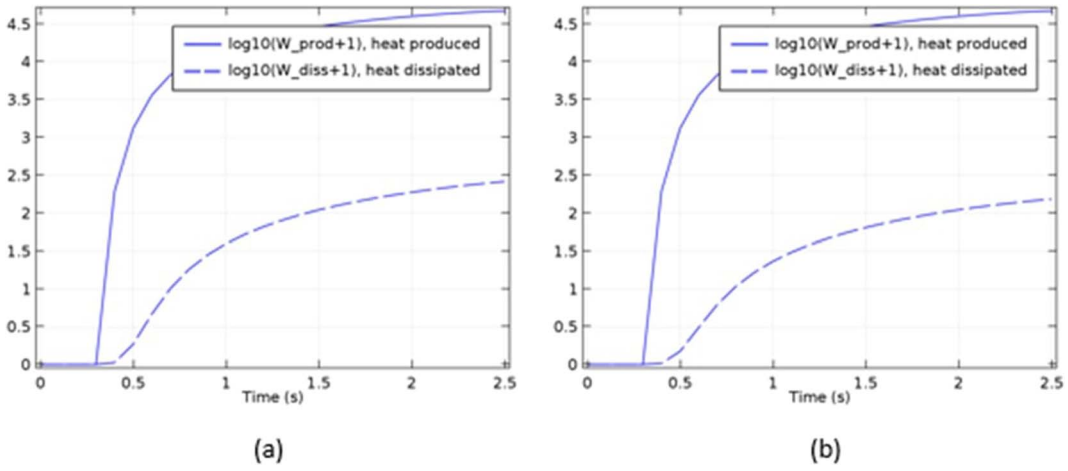

Figure 8. *Dissipated and produced heat (J) for 80 km/h. (**a**) Carbon-ceramic, (**b**) gray cast iron.*

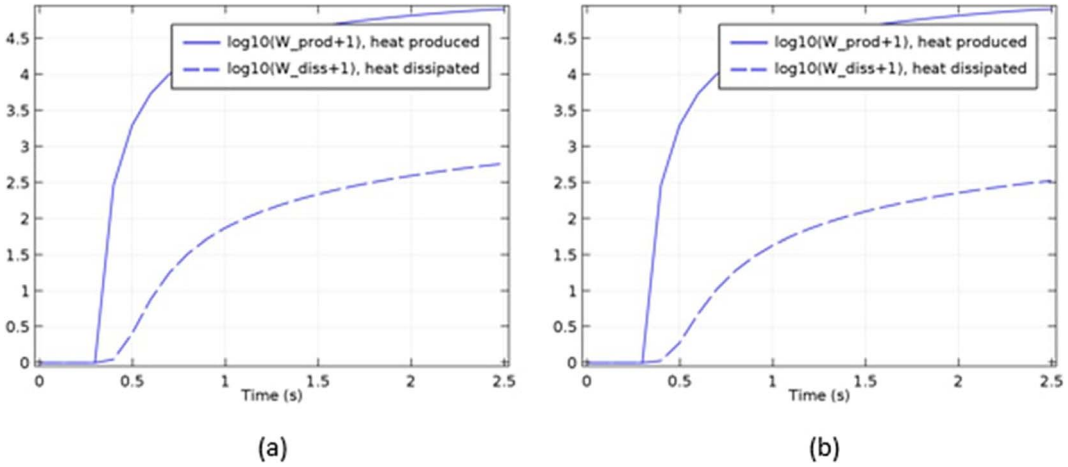

Figure 9. *Dissipated and produced heat (J) for 120 km/h. (**a**) Carbon-ceramic, (**b**) gray cast iron.*

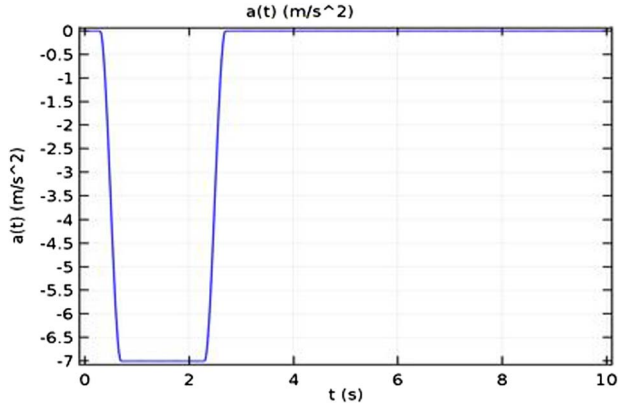

Figure 10. *Change of acceleration according to time.*

the disc material gray cast iron has been selected, 295–345, 300–420 and 300–500 K for the velocities of 50, 80 and 120 km/h, respectively. The maximum heat produced has been calculated for carbon-ceramic about 31621, 50117 and 79431 J for 50, 80 and 120 km/h, respectively. If the disc material gray cast iron has been selected, it has been observed that the produced heat values did not change. The maximum heat dissipated has been calculated for carbon-ceramic about 78, 250 and 561 J for 50, 80 and 120 km/h, respectively. If the disc material gray cast iron has been selected, 43, 158 and 315 J for 50, 80 and 120 km/h, respectively. When the coefficient of friction increases such as 0.5 and 0.7, there were no significant changes between the produced and consumed heat values. Therefore, it can be concluded that the coefficient of friction is not a significant parameter for the disc brake system.

4 CONCLUSIONS

In this study, a disc brake and pad have been modeled and analyzed as 3D by a multi-physics software. The surface temperatures of the disc brake and the pad have been investigated to examine the maximum reached temperatures affecting the stability of pad and brake disc material at elevated values. Thus, transferred heat

is a critical point of the contact surface. So, it has been computed heat generated on a disc and pad, and heat dissipated into the air versus time.

Thanks to this analysis, a specific disc brake and pad design can be tolerated before overheating. Also, parameters such as the amount of contact area and surface roughness of pad and brake disc affecting the heat generation and dissipation can be investigated. In future studies, it will be focused on design of various types of disc brakes with cooling channels.

REFERENCES

[1] Carmona S, Rouizi Y, Quemener O *et al.* Estimation of heat flux by using the reduced model and the adjoint method. Application to a disc brake rotating. *Int J Therm Sci* 2018;**131**:94–104.

[2] Vdovin A, Gustafsson M, Sebben S. A coupled approach for vehicle brake cooling performance simulations. *Int J Therm Sci* 2018;**132**:257–66.

[3] Yang Y, Chen W. A nonlinear inverse problem in estimating the heat flux of the disc in a disc brake system. *Appl Therm Eng* 2011;**31**:2439–48.

[4] Dhir D. Thermo-mechanical performance of automotive disc brakes. *Mater Today Proceed* 2018;**5**:1864–71.

[5] Yevtushenko AA, Grzes P. 3D FE model of frictional heating and wear with a mutual influence of the sliding velocity and temperature in a disc brake. *Int Commun Heat Mass Transfer* 2015;**62**:37–44.

[6] Aderghal N, Loulou T, Bouchoucha A, Rogeon P. Analytical and numerical calculation of surface temperature and thermal constriction resistance in transient dynamic strip contact. *Appl Therm Eng* 2011;**31**:1527–35.

[7] Kounas PS, Dimarogonas AD, Sandor GN. The distribution of friction heat between a stationary pin and a rotating cylinder. *Wear* 1972;**19**:415–24.

[8] Laraqi N, Baıri A, Segui L. Temperature and thermal resistance in frictional devices. *Appl Therm Eng* 2004;**24**:2567–81.

[9] Laraqi N. Contact temperature and flux partition coefficient of heat generated by dry friction between two solids. *Int J Heat Mass Transfer* 1992;**35**:3131–9.

[10] Moussa T, Garnier B, Pelay U *et al.* Heat transfer at the grinding interface between the glass plate and sintered diamond wheel. *Int J Therm Sci* 2016;**107**:89–95.

[11] Belhocine A, Bouchetara M. Thermal analysis of a solid disc brake. *Appl Therm Eng* 2012;**32**:59–67.

[12] Ghadimi B, Kowsary F, Khorami M. Thermal analysis of locomotive wheel-mounted disc brake. *Applied Thermal Engineering* 2013;**51**:948–52.

[13] Atmaca M, Girgin I, Ezgi C. CFD modelling of a diesel evaporator used in cell systems. *Int J Hydrog Energy* 2016;**41**:6004–12.

[14] Atmaca M, Çetin B, Yılmaz E. CFD analysis of unmanned aerial vehicles (UAV) moving in flocks. *Acta Physica Polonica A, vol* 2019;**135**:694–6.

[15] Atmaca M. Wind tunnel experiments and CFD simulations for gable-roof buildings with different roof slopes. *Acta Physica Polonica A, vol* 2019;**135**:690–3.

[16] Atmaca M, Ezgi C. Three-dimensional CFD modeling of a steam ejector. *Energ Source Part A Recov Util Environ Effects*, https://doi.org/10.1080/15567036.2019.1649326.